The influence of aluminum particles in a Hydroprocessed Vegetable Oil combustion

Inês A. S. Ferrão [*, 1,2,3], Miguel A. A. Mendes[2], Ana. S. O. H. Moita [3,4], André R. R. Silva [1]

[1] AEROG-LAETA, Universidade da Beira Interior, Covilhã, Portugal
[2] IDMEC-LAETA, Instituto Superior Técnico, Universidade de Lisboa, Lisboa, Portugal
[3] IN+-LARSyS, Instituto Superior Técnico, Universidade de Lisboa, Lisboa, Portugal
[4] CINAMIL, Portuguese Military Academy, Lisboa, Portugal

Abstract

The present work experimentally investigates single droplet combustion to understand the effect of aluminum particles when added to a biofuel. Experiments are carried out in a drop tube furnace to evaluate the influence of size and concentration of the aluminum particles. Two different sizes (40 nm and 5 µm) and two concentrations (0.5 and 1.0 wt.%) are studied at 1000 °C. The addition of aluminum particles improves biofuel combustion. Decreasing the particle size and increasing the particle concentration leads to a significant enhancement in the burning rate compared to the pure HVO. Micro-explosions are detected at the end of droplet lifetime when particles are added to biofuel.

Introduction

The addition of metal particles to liquid fuel is a topic that has been studied, focusing on the enhancement of conventional fuel performance. Aluminum, boron, carbon, iron in different sizes and concentrations have shown potential advantages when added to liquid fuel in several combustion systems.

In the last decades, studies were mostly based on micron-size particles however, through research and development of nanotechnology, a novel class of fuels arose. Nanoparticles in a range of 1-100 nm compared with micron-size particles present a higher specific surface area, higher reactivity, and the potential to store energy at the surface [1]. Stable nanoparticles in a conventional fuel could participate as a secondary energy carrier performing the following characteristics: increase volumetric energy density, enhance the catalytic activity, low ignition delay, higher ignition probability, higher burning rates, and reduction in soot and pollutant emissions [2]. The use of micron-size particles in several applications showed issues regarding clogging, rapid settlement, poor stability, and agglomeration [3]. Minimization of these effects is noticed with the addition of nanoparticles.

Diverse experimental studies were based on liquid fuel and micron-size particles of aluminum [4, 5] and boron [6], where disruptive burning phenomena were observed. These events, mostly named micro-explosions, occur when the primary droplet disintegrates, leading to secondary atomization, enhancing the effective fuel droplet size distribution, air-fuel mixing, and ultimately fuel efficiency [7]. The appearance of micro-explosions was also noticed for nanosuspensions. Javed et al. [8] evaluated the evaporation of kerosene + n-Al droplets in a suspended fiber under 400-800 ºC. The authors developed this experimental work using dense concentrations (2.5 wt.%, 5.0 wt.%, 7.0 wt.%), and micro-explosions were found. The results showed that by increasing the ambient temperature and particle concentration, the micro-explosions occur earlier in the droplet lifetime with much greater intensity. Wang et al. [9] studied the evaporation and micro-explosions of diesel and n-CeO_2. It was stated that by increasing the particle concentration, more nanoparticles are within the droplet leading to more local hotspots and heterogeneous nucleation sites. The findings can also be identified in many works regarding these subjects [10, 11].

Gan and Qiao [12] evaluated the combustion of nano and micron-size particles laden in ethanol and n-decane. Different stages were detected from the combustion of each fuel. In the combustion of n-decane + n-Al, five stages were spotted, namely, preheating, classical combustion, micro-explosion, surfactant flame, and aluminum droplet flame. However, for n-decane + m-Al, three stages, preheating, classical combustion, and micro-explosion were identified. According to the authors, the different visualization regarding the combustion of fuels is caused by the particle agglomeration during the process leading to a densely packed, impermeable shell for micron-size particles and a porous, more-uniformly distributed spherical aggregate for nano-size particles [12]. Jones et al. [3] performed an experimental study to evaluate aluminum and aluminum oxide combustion in biofuel (ethanol). The results showed that the amount of heat released from ethanol combustion increases almost linearly with n-Al concentration.

Recently, several efforts are being made to enhance biofuel combustion using nanoparticles. To change the current panorama of environmental concerns, the introduction of biofuels in the aeronautical industry might be a possible solution. It is imperative to reduce pollutant emissions, and alternative fuels have attracted interest due to the rapid growth of the aeronautical sector coupled with climate change. Biofuels can be derived from ATJ-SPK, SIP-SPK, FT-SPK, FT-SPK/A, HEFA, and other technologies. Several flights were already performed using biofuel as a blend or pure as its constituent. HVO is a HEFA biofuel, with a potential advantage in aviation, already adopted from Aeroméxico, Virgin Atlantic, and Japan Airlines. Patruno et al. [13] reported numerous situations where the research and effort to include biofuels in one of the most essential transportation sectors.

* Corresponding author: ines.ferrao@ubi.pt

The present work investigates the influence of different aluminum particle sizes (nano and micron) and concentrations (0.5 and 1.0 wt.%) added to a biofuel tested for aviation at a high ambient temperature. The addition of metal particles has been studied to liquid fuel, in particular for hydrocarbons. Consequently, the impact of these elements on biofuel combustion must be clarified. Additionally, the falling droplet method was employed in order to avoid any influence that supporting fiber may produce in droplet burning rate, disruptive burning phenomena, and others.

Experimental setup and procedure

Figure 1 shows a schematic experimental setup. This droplet combustion facility consists of an electrically heated drop tube furnace (DTF), an illumination set, an image acquisition system, and an injector device. Experiments are carried out in the drop tube furnace that allows the control of the wall temperature and oxygen concentration, achieving a maximum of 1200 ºC. The single droplet combustion occurs inside the vertical quartz tube with an inner diameter of 6.6 cm and a length of 82.6 cm placed at DTF. For the droplet visualization, two opposed rectangular windows with 2 cm width and 20 cm height are presented at the drop tube. The illumination set comprises a LED light and a diffusion glass to enhance the contrast and the accurate following of the droplet evaporation/burning process. An image acquisition system was placed in opposite windows from the illumination set to acquire the droplet combustion data. A CMOS high–speed camera (CR600×2, Optronics), coupled with a high magnification lens, was used to evaluate the single droplet combustion. The magnification lens is composed of a 6.5×Zoom, 12 mm FF, a 0.25×lens attachment, and a 2.0×short adapter, with a magnifying range of 0.35-2.25. The image acquisition was pursued with 1000 fps with a resolution of 1200×500 pixels and an exposure time of 1/13000 s. This acquisition system is connected to a computer, being the camera manually triggered. As shown in Figure 1, the air supply enters at the injector, with a flow rate of 5.7 L/min with a precision error of ± 2%. The air supply allows the formation of a proper environment for the droplet autoignition. The air is heated by the electric coils achieving the desire test temperature. The air is heated before the droplet injection, which occurs from a different inlet. The droplet injection occurs with the aid of a syringe pump, frequency generator and droplet generator. The droplet generator is a TSI device placed at the top of the DTF. A pinhole with a diameter of 200 µm generates a stream of droplets. The fuel is supplied by a syringe with a volume of 50 mL coupled to the syringe pump. The droplets are regulated by the syringe pump and frequency generator with the following operating conditions: 2.1 kHz and a flow rate of 1.3 mL/min. A stream of droplets with an initial diameter of 250 ± 8 µm is released and to guarantee the space/time between droplets, a rotating disk is used to ensure the analysis of single droplet combustion. The rotating disk is placed between the droplet generator and DTF, with a diameter of 12 cm with a rotational speed of 1200 rpm. A slot is presented at the rotating disk with 1 cm x 1cm, allowing the droplet entrance to the quartz tube. The image data processing was performed in ImageJ software to evaluate the droplet size evolution, burning rate, among others. The droplet outline is marked through the brightness gradient, allowing the droplet characterization. For the optical configuration used in this work, the pixel size was 12 µm.

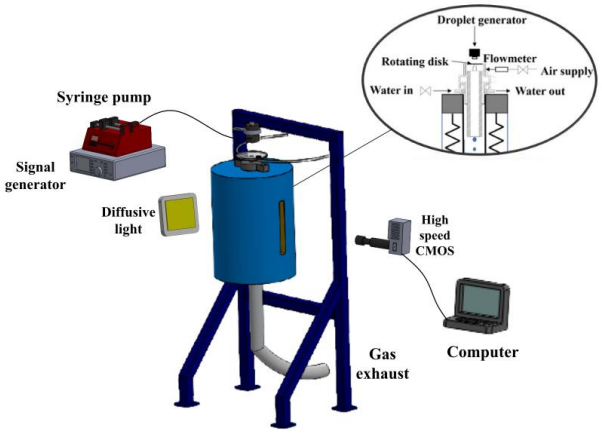

Figure 1 - Experimental setup.

The ambient temperature tested was 1000 ºC. Five fuels were investigated, including pure HVO, for comparison purposes. This biofuel is a NExBTL sourced by NESTE. Due to HVO chemical composition, approximately similar to fossil fuels can be used as a drop-in fuel, through blends, or as a neat product at 100% concentration. Table 1 shows the biofuel properties used as the base fuel [14, 15].

Table 1 - Biofuel properties [14, 15].

Parameter	HVO
Density (Kg/m^3) (at 20 ºC)	780.6
Surface tension (N/m) (at 20 ºC)	0.0265
Kinematic viscosity (mm^2/s) (at 25 ºC)	4.33
Sulfur (wt.%)	0.09
Aromatics (wt.%)	0
Flash point (ºC)	99
Final boiling point (ºC)	308
Cloud point (ºC)	-30
Distillation 10 vol.% (ºC)	262
Lower heating value (Mj/Kg)	43.9
Higher heating value (Mj/Kg)	47.1

As mentioned above, the addition of energetic metal particles influences the combustion of liquid fuel. The addition of aluminum particles has been studied and used additives in propellants and explosives. Aluminum is an abundant element, an excellent conductor of heat, low toxicity, relatively reduced cost, and high combustion energy [16].

To evaluate the influence of size and concentration of the aluminum particles added to HVO, two different sizes (40 nm and 5 µm) and two concentrations (0.5 wt.% and 1.0 wt.%) were tested. Table 2 shows the properties of HVO with aluminum nano (HVO + n-Al) and micron (HVO + m-Al) particles. The density was determined with the pycnometer method, and the surface tension was measured at room temperature (20 ± 3 °C) with an optical tensiometer THETA (Attension). A pendant drop method was employed, and a detailed description regarding this procedure can be found in [17]. The viscosity was measured with a rheometer (TA instruments ARI 500 ex), at ambient temperature, with an accuracy of ± 5%.

Table 2 - Properties of biofuel with the addition of nano and micron particles.

	HVO + n-Al 40 nm		HVO + m-Al 5 µm	
Particle concentration (wt.%)	0.5	1.0	0.5	1.0
Density (Kg/m^3)	771.4	773.2	774.5	770.9
Surface tension (N/m)	0.0265	0.0266	0.0265	0.0267
Viscosity (Pa.s)	0.02	0.055	0.035	0.059

To evaluate the addition of aluminum particles to an alternative fuel, a stability study was performed. The purpose of this analysis was to ensure that the fuel is stable with a low level of agglomeration during the experiments and to provide a promising fuel. Subsequently, a strict procedure was adopted. Firstly, the biofuel was mixed with the particles using a magnetic stirrer for 20 minutes. Then, it was sonicated in an ice bath for approximately 30 minutes. After the sonication, the fuels were evaluated through visualization for several hours and days. The results reveal that increasing the particle size and concentration, the fuel stability is affected. Hence HVO + m-Al (1.0 wt.%) presents stable approximately 2 hours.
On the other hand, HVO + n-Al (0.5 wt.%) display no evident sedimentation for almost 24 hours. According to Das et al. [18], the stability of fuels using particles, specifically nanoparticles, reduces the size tends to coagulate less, leading to reducing particle setting probability. To enhance biofuel stability with nano and micron particles, the surfactant addition is essential in future works.

Results and discussion

In this section, the visualization and description of single droplet combustion will be addressed. Figure 2 shows a sequence of images regarding the combustion of pure HVO at a temperature of 1000 ºC. When the droplet enters the quartz tube, a flame at the droplet wake with low intensity is formed. Through the descent movement, the droplet diameter shrinks. The droplet diameter regression is visualized with the aid of a high-speed camera that follows the droplet trajectory. During its stages of evaporation/combustion, no micro-explosions and puffing were detected. The visualization of droplet size regression along with the time is displayed in Figure 2, where no disruptive burning phenomena are spotted.

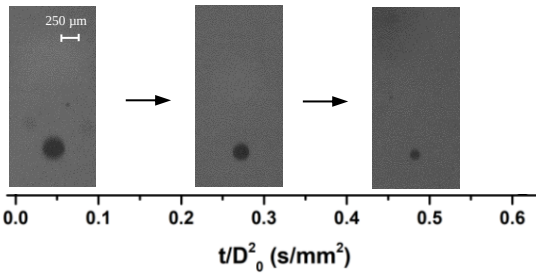

Figure 2 - Sequence of images regarding pure HVO droplets with an initial droplet diameter of 250 µm at T = 1000 ºC and atmospheric pressure.

Figure 3 shows an analysis of pure HVO based on the D^2-Law, to better understand the influence of the ambient temperature (T = 1000 ºC) on the biofuel falling droplet. Figure 3 shows the normalized droplet diameter as a function of the normalized time. The results show that the pure HVO is in good agreement with the D^2 law, which predicts that the normalized square diameter decreases linearly with time with a nearly constant slope, denominated by burning rate, which will be detailed described in the following paragraphs. The initial droplet diameter is represented by D_0 and the initial time corresponds to the droplet entering the quartz tube.

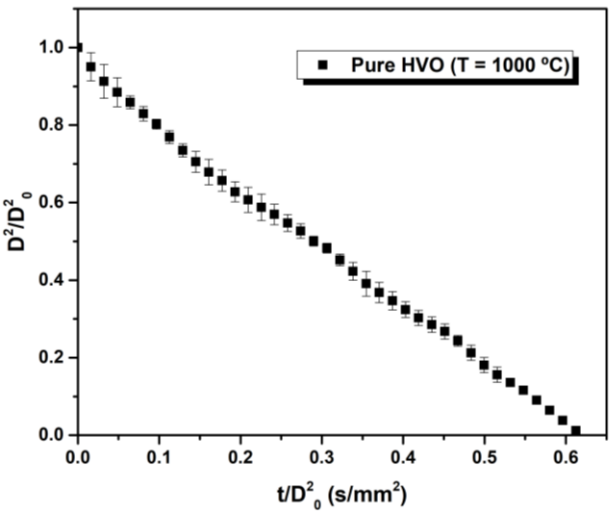

Figure 3 – Droplet size evolution of pure HVO at T = 1000 ºC and atmospheric pressure with an initial droplet diameter of 250 µm.

In order to smoothen the droplet size evolution curves, a three-point moving average was used. In this way, the instability provided by the analysis will be

softened. In order to hinder any inaccurate results due to the considerably small diameter of the droplet at the end of the droplet lifetime, the experimental data were analyzed and treated until $D^2/D^2_0 = 0.2$. Then, the droplet size evolution curve was complete by counting the number of frames until the end of the droplet lifetime and fitting with the burning rate value. The development of droplet size evolution was previously evaluated through statistical analysis to ensure that the combustion characteristics were independent of the sample's size. Thus, it was confirmed that using 40 droplets for the D^2 law curve and burning rate graphics does not affect the results' accuracy. As previously mentioned, no disruptive burning phenomena were detected during the evaporation/combustion of pure HVO, as demonstrated in Figure 3. Overall, the pure HVO evaporates and burns as a fully liquid droplet.

To evaluate the effect of the addition of aluminum particles in nano and micron scale to biofuel, the falling droplets were exposed to a high ambient temperature (T = 1000 ºC) in a drop tube furnace. Figure 4 shows the droplet size evolution mentioned above. Comparing Figure 4 with the droplet size evolution of pure HVO displayed in Figure 3, the addition of particles alters the droplet dynamics during the evaporation/combustion process regardless of the particle size and concentration.

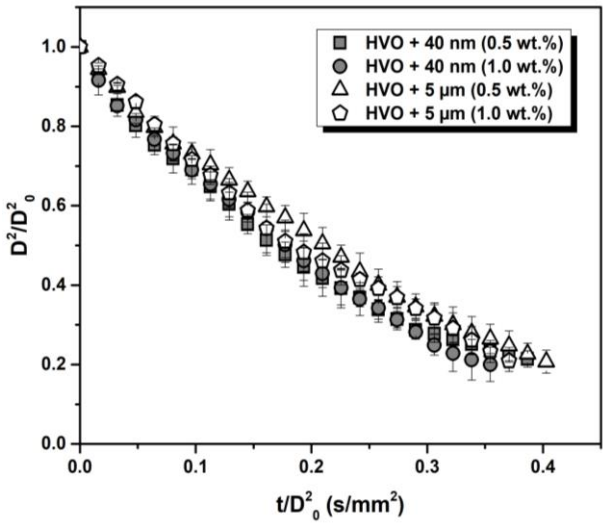

Figure 4 - Droplet size evolution at T = 1000 ºC and atmospheric pressure with an initial droplet diameter of D_0 250 µm of the following fuels:

- HVO + n-Al 40 nm (0.5 wt. %).
- HVO + n-Al 40 nm (1.0 wt. %).
- HVO + m-Al 5 µm (0.5 wt. %).
- HVO + m-Al 5 µm (1.0 wt. %).

For the pure HVO droplets, the D^2-law was obeyed. However, when particles were added to the biofuel, a curvature was depicted for all the fuels tested, as shown in Figure 4. Similar to Figure 3, a three-point moving average was employed, and the experimental data were added to Figure 4 until $D^2/D^2_0 = 0.2$. The gray symbols represent the nanofuels composed of 40 nm with two particle concentrations, on the other hand, the biofuel with micron size particles (5 µm) and two particle concentrations correspond to the white symbols.

Firstly, at the beginning of the droplet size evolution of each curve, the droplet diameter is considerably reduced along with time. However, approximately at $t/D^2_0 = 0.3$, a slight variation in the curves indicates that the evaporation rate decreases as time evolves. When the liquid phase is evaporating, the particles that remain within the droplet tend to affect the droplet evaporation, which influences the droplet size evolution, as shown in Figure 4. Due to this, the particles hinder or even preclude the evaporation, leading to a non-linearity at the end of the droplet lifetime. This fact is observed regardless of the particle size and concentration. It is essential to highlight that, specifically until $t/D^2_0 = 0.3$, no disruptive burning phenomena were detected during this stage.

Figure 5 shows a sequence of images of HVO + 40 nm (1.0 wt. %) and HVO + 5 µm (1.0 wt. %). As already mentioned, a flame at the droplet wake appears when the droplet enters the quartz tube. As the time evolves, for each fuel with different particle size, the droplet diameter reduces considerably as expected and discussed in Figure 4. Afterward, for HVO + 40 nm (1.0 wt. %), an alteration in the droplet appearance indicates the onset of a micro-explosion at t = 37 ms. At this moment, the primary droplet disintegrates, and particle agglomerates are expelled in several directions, as can be seen at the instant t = 38 ms. As a consequence of these particle agglomerates release, various intense bright spots appear pronouncing the aluminum combustion. The end of this event occurs when residue that remains ascends along with a smoke tail in the flow field. A similar explanation is given for HVO + 5 µm (1.0 wt. %). As the droplet is exposed to the high ambient temperature, its diameter reduces. Then, at t = 40 ms, a disruption of the droplet is detected. Thus, as observed in the previous case, innumerous agglomerates are ejected, which ignites promoting aluminum combustion. Micro-explosions are considered secondary atomization that enhances the air/fuel mixing, leading to decreased droplet lifetime and improved combustion efficiency. It should be pointed out that micro-explosions only occur when particles are added to the biofuel. The probability of a micro-explosion occurring is 100%, regardless of the particle size and concentration in the present work. Additionally, the micro-explosions determine the end of the droplet lifetime.

The visualization of these droplets mainly composed of HVO with different sizes and similar concentrations demonstrated that increasing the particle size promotes a later micro-explosion occurrence. The onset of the disruptive burning phenomena appears when the liquid fuel is consumed and the particle concentration within the droplet increases. Then, a local hot spot can arise and promote the disruption of the primary droplet, leading to

micro-explosion and ejection of intense bright spots in several directions.

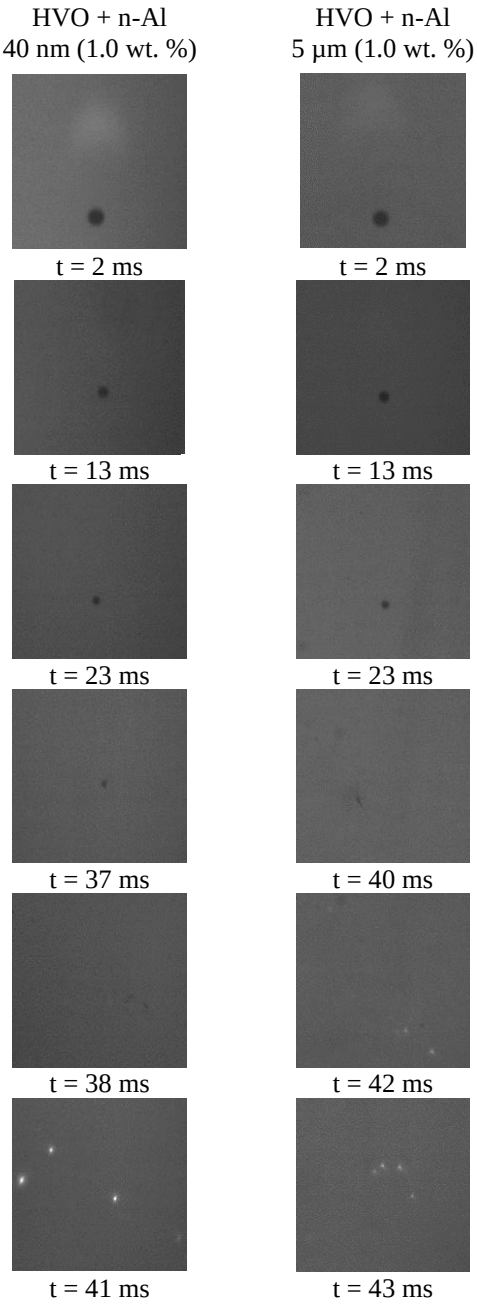

Figure 5 - Sequence of images regarding HVO + 40 nm (1.0 wt. %) and HVO + 5 µm (1.0 wt. %) with an initial droplet diameter of 250 µm at T = 1000 ºC and atmospheric pressure.

The presence of particles in the liquid fuel affects the evaporation rate. Figure 6 shows burning rate evolution, comparing pure HVO and HVO + 40 nm (1.0 wt. %). The results show that the pure HVO presents an approximately constant burning rate as time evolves. On the contrary, for the nanofuel HVO + 40 nm (1.0 wt. %) a considerably high burning rate is represented at the beginning of its lifetime. As a consequence of the increase in the particle concentration within the droplet, the temporal evolution of the burning rate tends to decrease and become even smaller than the pure HVO at the end of the lifetime, approximately at $t/D^2_0 = 0.3$.

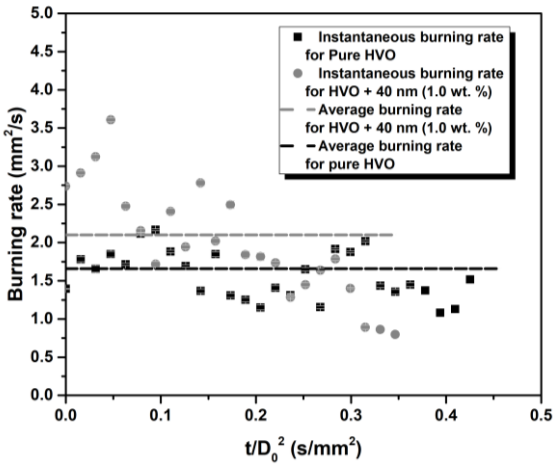

Figure 6 - Temporal evolution of burning rate and average burning rate for the pure HVO and HVO + 40 nm (1.0 wt. %) with an initial droplet diameter of 250 µm at T = 1000 ºC and atmospheric pressure.

As previously mentioned, the particles that remain within the droplet difficult the evaporation, resulting in a decrease of the burning rate at the end of the lifetime. Figure 7 shows the burning rate to evaluate and compare all the fuels tested in the present work. This analysis was achieved using 40 droplets and was determined by $K = -d(D^2)/dt$, being K the average burning rate.

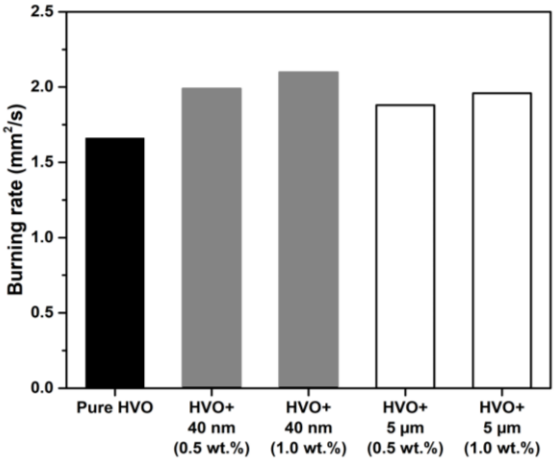

Figure 7 - Burning rate.

The addition of aluminum particles to the biofuel enhances the burning rate regardless of the particle size and concentration at an ambient temperature of T = 1000 ºC in a contactless environment. In the present work, the burning rate of pure HVO is lower than that obtained for other fuels. Comparing the nano and micron size particles, it can be stated that reducing the particle size increases the burning rate, regardless of the particle concentration. It can be affirmed that, for a constant particle concentration, decreasing the particle size leads to a larger wet surface area of the particles, leading to an enhancement in the evaporation rate. Regarding the

particle concentration, the burning rate decrease as the concentration decrease, regardless of the particle size.

Conclusions

The present work evaluates the combustion of a falling single droplet with an ambient temperature of T = 1000 ºC. The effect of particle size and concentration, when added to biofuel, was investigated, and the main conclusions are the following:

- When the droplet enters the quartz tube, a flame at the wake of the droplet appears. A pure biofuel and four fuels with particles were investigated, and the pure HVO was the one that follows the D^2-Law.
- The addition of particles, regardless of their size and concentration, enhances the biofuel combustion performance. Pure HVO presents the lowest burning rate, and HVO + 40 nm (1.0 wt. %) presents the highest value.
- Micro-explosions appear for all the fuels, with particles pronouncing the end of the droplet lifetime. In general, the occurrence of these disruptive burning phenomena occurs earlier for HVO + 40 nm, more concretely for the fuels with smaller size.

Acknowledgments

Inês Ferrão acknowledges Fundação para a Ciência e Tecnologia (FCT) for the provision of Ph.D scholarship with the reference SFRH/BD/144688/2019. The present work was performed under the scope of the Laboratório Associado em Energia, Transportes e Aeronáutica (LAETA) and Laboratório de Robótica e Sistemas de Engenharia (LARSyS) activities and it was supported by Fundação para a Ciência e Tecnologia (FCT) through the projects numbers UIDB/50022/2020 and UIDB/50009/2020. Authors would also like to acknowledge Fundação para a Ciência e Tecnologia for partially supporting this work through project PTDC/EME-SIS/3017.

References

[1] Y. Gan, L. Qian, Radiation-Enhanced Evaporation of Ethanol Fuel Containing Suspended Metal Nanoparticles, International Journal of Heat and Mass Transfer, 55 (2012), 5777–5782.

[2] S. Basu, A. Miglani, Combustion and Heat Transfer Characteristics of Nanofluid Fuel Droplets: A Short Review, International Journal of Heat and Mass Transfer, (2016) 482–503.

[3] M, Jones, C. H. Li, A. Afjeh, G. Peterson, Experimental Study of Combustion Characteristics of Nanoscale Metal and Metal Oxide Additives in Biofuel (Ethanol), Nanoscale Research Letters, 6 (2011).

[4] B. Young, S. W. Baek, J. H. Cho, Microexplosion of Aluminum Slurry Droplets (1999).

[5] S. C. Wong, A. C. Lin, Microexplosion Mechanisms of Aluminum/Carbon Slurry Droplets, 89 (1992).

[6] F. Takahashi, I. J. Heilweil, F. L. Dryer, Disruptive Burning Mechanism of Free Slurry Droplets, Combustion Science and Technology, 65, (1989) 151–165.

[7] S. S. Sazhin, O. Rybdylova, C. Crua, M. Heikal, M. A. Ismael, Z. Nissar, A. R. B. A, Aziz, A Simple Model for Puffing/Micro-Explosions in Water-Fuel Emulsion Droplets. International Journal of Heat and Mass Transfer, 131 (2019) 815–821.

[8] I. Javed, S. W. Baek, K. Waheed, Effects of Dense Concentrations of Aluminum Nanoparticles on the Evaporation Behavior of Kerosene Droplet at Elevated Temperatures: The Phenomenon of Microexplosion, Experimental Thermal and Fluid Science, 56 (2014) 33–44.

[9] J. Wang, X. Qiao, D. Ju, L. Wang, C. Sun, Experimental Study on the Evaporation and Micro-Explosion Characteristics of Nanofuel Droplet at Dilute Concentrations, Energy 183 (2019) 149–159.

[10] Sim, H. S.; Plascencia, M. A.; Vargas, A.; Bennewitz, J. W.; Smith, O. I.; Karagozian, A. R. Effects of Inert and Energetic Nanoparticles on Burning Liquid Ethanol Droplets. Combustion Science and Technology 2019, 191 (7), 1079–1100.

[11] S. Tanvir, L. Qiao, Effect of Addition of Energetic Nanoparticles on Droplet-Burning Rate of Liquid Fuels, In Journal of Propulsion and Power, American Institute of Aeronautics and Astronautics Inc., 31 (2015) 408–415.

[12] Y. Gan, L. Qiao, Combustion Characteristics of Fuel Droplets with Addition of Nano and Micron-Sized Aluminum Particles, Combustion and Flame 158 (2011) 354–368.

[13] A. Patruno, V. Amicarelli, G. Lagioia, Aviation Fuel Evolution: A review (2016).

[14] N. Nylund, K. Erkkilä, M. Ahtiainen, T. Murtonen, P. Saikkonen, A. Amberla, H, Aatola, Optimized Usage of NExBTL Renewable Diesel Fuel. OPTIBIO (2011).

[15] A. Dimitriadis, T. Seljak, R. Vihar, U. Žvar Baškovič, A. Dimaratos, S. Bezergianni, Z. Samaras, T. Katrašnik, Improving PM-NOx Trade-off with Paraffinic Fuels: A Study towards Diesel Engine Optimization with HVO, Fuel, 265 (2020).

[16] W. Hao, G. Li, L. Niu, R. Gou, C. Zhang, Molecular Dynamics Insight into the Evolution of Al Nanoparticles in the Thermal Decomposition of Energetic Materials. Journal of Physical Chemistry C, 124 (2020) 10783–10792.

[17] A. S. Moita, C. Laurência, J. A. Ramos, D. M. F. Prazeres, A. L. N. Moreira, Dynamics of droplets of biological fluids on smooth superhydrophobic surfaces under electrostatic actuation, Journal of Bionic Engineering, 13 (2016) 220-234.

[18] S. K. Das, N. Putra, P. Thiesen, W. Roetzel, Temperature Dependence of Thermal Conductivity Enhancement for Nanofluids, Journal of Heat Transfer, 125, (2003) 567–574.